Solar and Heat Pump Systems: parallel vs series configurations analysis

J. Vega[1]*, C. Cuevas[2]

(1) Departamento de Ingeniería Mecánica - Universidad de Concepción

Edmundo Larenas 219 - Concepción – Chile

(2) Departamento de Ingeniería Mecánica - Universidad de Concepción

Edmundo Larenas 219 - Concepción – Chile

1. ABSTRACT

This paper presents simulations of a Solar and Heat pump System (SHP) system for Domestic Hot Water (DHW) preparation. Two system configurations are designed for covering the heat demand. These, can switch between parallel and series operation. Thus, Configuration "A" consists in using a heat pump with two evaporators that alternate: one to work as an air-to-water heat pump (HP) and the other to operate as a water-to-water HP using the solar collector's (SC) heat. Configuration "B" implements a heat exchanger in the air-to-water HP that can pre-heat the air, using solar energy. These system configurations are modelled in the TRNSYS 17 environment for evaluating system's performance in different climates and with different SCs. The control system applies a switching criterion between parallel or series operation modes, based primarily on the available solar irradiation. Results show that individual performance figures of the HP and the SCs increase. Nonetheless, the Seasonal Performance Factor (SPF) of the overall system decreases in most case studies (5.58 to 4.55 in the worst case). It is emphasized that the applied switching criterion does not force the SCs to increase their operational time by cooling them with the HP. In consequence, there is still potential solar energy unused that the series operation could seize.

Keywords: Solar and heat pump systems, series configuration, parallel configuration, control systems

2. INTRODUCTION

In central and southern Chile, residential heating systems are mainly based on wood, paraffin or liquefied petroleum gas stoves. Among these, wood is the most frequently used fuel because of its lower price and wide availability. Unfortunately, the combustion of wood is the main source of air pollution during the winter period, with several cities declared as saturated by airborne pollution. In the case of the domestic hot water, it is mainly heated by the combustion of liquefied petroleum gas or natural gas. Even if for this case the pollution concernf is less severe, there is still a constraint related to the cost of the fuels, proven to be highly sensitive to past energy crises. These problems motivate the present study to evaluate the performance of alternative, more efficient, and less contaminant technologies like heat pumps combined with solar collectors. These are known as Solar and Heat Pump Systems (SHP systems).

SHP systems have been widely studied in the literature, especially by IEA SHC Task 44. As said, they combine heat pumps with solar thermal technology, typically solar thermal collectors, to supply energy demands on Domestic Hot Water (DHW) and Space Heating (SH). To achieve this , these systems usually need an energy storage: hot water stratified storage tanks appear as the more frequent and market available for this function. Nonetheless, multiple systems architectures can result in combining these components. One way to categorize them, used by Task 44, is according to the interaction of their components, which was fully described by Ruschenburg et al. (2013). Thus, three main configurations are defined: parallel, series and regenerative. The configuration is denoted as parallel if the SC and the HP independently supply useful energy. Second, when collectors act as the heat source for the heat pump, either as exclusive or additional source, the configuration is denoted as series. Last, if the solar energy is used to warm and maintain the main source of the heat pump, usually the ground, it is denoted as regenerative. The energy performance of the SHP systems depends on several variables such as the building characteristics, the heat pump components, the solar radiation, the ambient conditions, the energy demand schedules, and of course, the overall systems components interaction. Regarding the last, series configuration concept is of interest. It has been created to boost the individual performance of both solar collectors and heat pump. In fact, if solar collectors are the HP's heat source, then they are chilled by it. Thus, at lower operational temperatures, they improve their performance by reducing their convection heat losses to the ambient. On its side, heat pump's Coefficient of Performance (COP) benefits from working with a higher temperature heat source than the air or ground would be. These are the foundations that motivate the present paper.

Most of the SHP systems performance analyses are developed using modelling and simulations during a representative period. For the modelling, different kinds of approaches are proposed in the literature, classified by Hadorn J.C (2015). Semi-empirical black box models are the most popular approaches used to model conventional systems by giving sufficiently accurate results. These models are executed in programs like TRNSYS, Energy-Plus, ESP-r, Insel or Matlab, among others. Most of these component models are validated and it is assumed that the simulation of the overall system is thus correct. Nonetheless, some authors warn that these SHP systems simulated performance is rarely validated experimentally. This is remarked by Banister C. and Collins M. (2015) in their literature survey. This may be explained by the complexity of the systems and the costs associated to the instrumentation and to the measurements campaign. Nonetheless, some studies are found with in-field measurements and good model validation. For example, Fraga et al. (2017) validated the simulations for a SHP system including an ice storage using one-year measurements from a pilot plant. On their side, Liu et al. (2014) have done in-field measurements to determine a high-capacity SHP system performance for an office building, and then used TRNSYS simulations to optimize its operational behaviour.

Regarding the expected results of a SHP simulation, sizing of the equipment is fundamental. In particular, solar energy contribution will have great impact on the system Seasonal Performance Factor (SPF_{syst}), the most important figure to compare. It is found that increasing the total solar collector area is most likely going to increase SPF_{syst}, although the decrease of the total electric consumption is asymptotic as a function of the SPF_{syst} increase, as shown by Fraga et al. (2017). Then, in reasonably sized systems, the limit to the total solar collar collector's area will always respond to an economic criterion. For the evaluated systems in the climate of Geneva, the mentioned author concluded that for Geneva's weather, 3 m^2 of solar collector per kW of heat pump capacity is a good compromise between system size and system performance.

There is abundant literature regarding parallel systems. Systematic work was done by Carbonell et al. (2014) to analyse potential electricity savings of parallel SHP systems compared to simple Air-Source Heat Pumps (ASHP) and Ground-Source Heat Pumps (GSHP). Work has also been done to investigate parallel SHP systems performance with improvements in the heat pump's cycle, such as the case of ASHP studied by Poppi et al. (2016). They developed a theoretical analysis using TRNSYS for two different climates, using variable speed heat pumps, vapour injection compressors, condensers integrated in the storage tank, between others.

Regarding the study of series configuration systems, some are just heat-pump-focused. Sun et al. (2015) compared an air-source heat pump with a solar source heat pump in the highly heterogeneous climate of Shanghai, China. In their case study, SPF_{HP} was higher using series configuration, which is what should be expected. Others focus their conclusions more in SC's performance increase when chilled by the heat pump, such as Sterling et al. (2012). They also studied solar source heat pumps for DHW, predicting a solar fraction increase from 58% to 67%. Tzivanidis et al. (2016) developed a parametric analysis in TRNSYS for three different heating systems: a solar system, an ASHP and a solar source heat pump. They concluded the solar source heat pump was more convenient than the air-source one. Nonetheless, no parallel configuration was evaluated to compare its performance. Other complex systems using solar source heat pumps have been evaluated with measurements and simulations, but with no direct comparison between parallel and series configuration (Liu et al., 2014). Then, there are some innovative studies on series SHP systems. Banister and Collins [13] proposed to improve a classical series system with a dual tank solar source heat pump, which allowed to reduce the energy consumption from 60% to 69% when this system was used with a solar collector area of 7.5 m^2. They also noticed in their literature survey that the general conclusion of solar assisted heat pump systems is that energy savings exist in comparison to traditional solar domestic hot water systems. Other novel system was developed by He et al. [14] in which a solar façade loop-heat-pipe was used as source for a HP. The authors simulated the performance and compared their results with a test rig, concluding an average thermal efficiency of the solar façade of 71% and an average COP of 4.93 that could reach up to 6.14.

There is few but existing literature that compares parallel and series configuration directly. Lerch et al. (2015) compared several SHP systems for heating and DHW; studying different kinds of series configurations, including ice storages, air preheating by solar energy and refrigerant heating by solar energy after the heat pump's evaporator. Compared to a classical parallel configuration, the results showed little system performance increase. In addition, using unglazed collectors as source for the heat pumps, the system required to double the collector's aperture area to achieve a similar system performance.

Systems that work in a series configuration only have a disadvantage: if there is a heat demand when there is not enough solar radiation, the heat pump's performance would be low because of poor heat exchange between the solar collectors and ambient air. Thus, dual source heat pumps are interesting since they search to combine the best features of parallel and series configuration SHP systems. In these, the heat pump can switch between using solar energy or, for example, air source energy. Then, the control system for the heat pump's operation mode switching criterion is of high interest. Kaygusus K. (1995), managed to improve the overall system performance using an air-source and solar-source heat pump in the climate of Trabzon, Turkey. For this, the author implemented an operation mode switch criterion based on the collector's outlet temperature. Lazarrin M. (2012) deepened Kaygusus's work stufdying ground source heat pumps coupled with solar collectors, both systems with the capability to work in a series mode. He concluded that in series mode, as expected, higher COP can be achieved, but there is often a lower free (air+solar or ground+solar) energy fraction, requiring auxiliary energy more frequently. On the other hand, Haller et al. (2011) described the potential of these dual source configurations. The authors also focused in comparing a dual air-source and solar-source heat pump. It is shown by theoretical analysis and dynamic system simulations that, there is a limit for the solar irradiation on the collector field above which using collector heat for the evaporator of the heat pump instead of using it directly is not advantageous. This irradiation limit (G_{lim}) depends on the characteristic performance curves of the solar collector and of the heat pump, as well as on the temperature conditions of the heat sources and sinks. This can be used as a criterion for switching between parallel and series operation mode. Thus, the authors concluded there is a high potential in improving the system's performance taking advantage of the additional running times the collectors gain when chilled by the heat pump. It is important to notice that Haller's criteria for switching between parallel and series is based on idealized and steady state conditions. Hadorn J.C (2015) warned that this does not consider the transient effect of thermal capacitances.

The present work is inspired by these last conclusions. The objective is to study SHP systems that can conmute between parallel and series mode of operation. The hypothesis, derived from Haller et al., consists in assuming that there exists a solar irradiation value G_{lim} below which a SHP system benefits the most if it operates in series mode exclusively. This is assumed valid for every combination of flow temperature of the heat demand and ambient temperature. This hypothesis is applied to two different system configurations. The hypothesis also implies that if in any of the previous mentioned SHP systems a control system could switch between parallel and series operation based on the available solar irradiation, then the SPF_{syst} would be optimized. On the other side, a certain parallel system will have a determined amount of time in which solar collectors effectively use available solar energy. So, could such the beforementioned control strategy be beneficial without modifying the solar collectors runtimes? For testing this thesis, SHP systems capable of switching its operation mode will be designed, modelled and simulated in TRNSYS to assess their performance in typical meteorological years in 3 Chilean cities. The case studies are derived from the heat demand of DHW and SH a medium rise Chilean residential building that has already been used by Vega et al. (2018) for assessing SHP systems performance for simple parallel systems. Nonetheless, the present paper focus its study just in the DHW heat demand.

3. METHODOLOGY

A system for DHW coverage of a mid-rise residential building is assessed. The selected heat demand to cover permits to evaluate the thesis in a somewhat high temperature load and with high component's thermal capacitance. High thermal capacitance on the Hot Water Storage Tank (HWST) and SCs, allows covering Hadorn's concerns on transient effects in the operation mode switching criterion. The system is tested in two different configurations, denoted as A and B, each of them capable of operating in parallel or series mode. Configuration A consists in a double evaporator HP, that can use as its energy source ambient air or solar energy from the SC. On the other hand, B configuration's series operation consists in using solar heat to warm the air passing though the heat pump. A simple solar radiation based criterion is applied based on different fixed solar irradiations value, $G_{lim,control}$, below which series operation will be activated. Thus, several numerical simulation to determine system's performance are carried on with different values of $G_{lim,control}$ set aiming to find an irradiation value that would switch parallel and series operation in an beneficial way.

3.1. Simulations boundary conditions

Regarding the boundary conditions of the simulations to test the studied systems, they can be divided in two: climate conditions and heat demand profiles. It is aimed to get valuable conclusions and performance indicators for the Chilean context. Then, to fully describe simulations boundary conditions, selected city weathers will first be presented, then, the heat loads and profiles that the SHP system seek to cover.

3.1.1. Climate boundary conditions.

The system covering the heat demand is evaluated in 3 different Chilean cities. First, Santiago is chosen for being the most populated city in Chile. Then, two cities are selected in the southern, and thus colder, regions of Chile: Concepcion, and Puerto Montt. Using different climate conditions is of interest because an ideal $G_{lim,control}$ will depend on ambient temperature and will also be reached at lower frequencies in southern cities. The characteristics of selected climate data are summarized in Table 1.

Table 1: Chilean thermal zone classification (MINVU, 2007), Köppen climate classification (Weatherbase, 2018) and climate data (Meteonorm, 2017) that characterize the selected weather

	Santiago	**Concepción**	**Puerto Montt**
Chilean thermal zone classification	Zone 1	Zone 4	Zone 6
Köppen climate classification	Csb (Mediterranean climate) bordering BSk (semi-arid climate)	Csb (mediterranean climate)	Cfb (marine west coast climate)
Average annual temperature	14.7 °C	12.5 °C	10.2 °C
Anual solar irradiation on a horizontal surface	1739 *kWh/m2*	1493 *kWh/m2*	1166 *kWh/m2*

3.1.2. Heat loads and energy demand profile.

A typical mid-rise building of Concepcion, Chile, is chosen for modelling its DHW heat load. The residential building with a total of 78 apartments, 13.2 m total high and located in Concepción, southern Chile. More details concerning its design and space heating related data are presented by Vega et al. (2018). The DHW profile demand used in this analysis is the one recommended by the ASHRAE Standard 90.2, while the total daily water consumption is estimated in 25270 litters according to ASPE. The DHW consumption temperature is defined as 48 °C. The resulting daily consumption is shown in Figure 1. Using the selected meteorological data, the heat load required to keep the internal energy of a DHW hot water storage tank during the whole year is presented in Table 2.

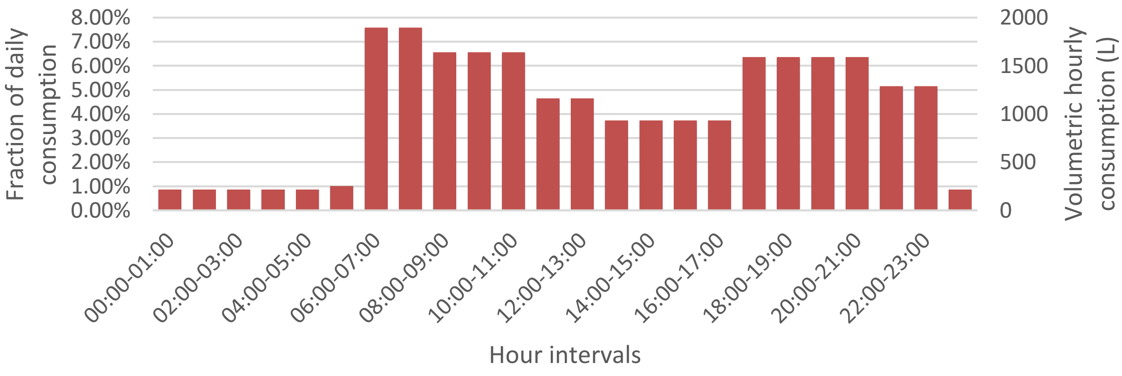

Figure 1: Daily consumption of DHW of the studied residential building.

Table 2: Heat load for DHW preparation in each assesed climate.

	Santiago	***Concepción***	***Puerto Montt***
Maximum capacity demand	*73.5 kW*	*76.6 kW*	*84.0 kW*
Annual energy demand	*315 890 kWh*	*350 720 kWh*	*388 610 kWh*

4. DESIGN AND MODELLING OF THE SHP SYSTEMS.

4.1. Overall design and system configurations.

Two different SHP system layouts are designed and modelled in TRNSYS: the SHP system in its A and B configurations. Besides testing these layouts in different climates and control system configurations, the use of two different types of solar collectors is proposed: Evacuated Tubes Collectors (ETCs) and Unglazed Collectors (UC). From a certain point of view, these collectors' performance profiles are opposed. ETC have a low optic performance, but low convective heat losses when they operate at higher temperatures. In contrary, UC can have a higher thermal efficiency if they are work at low temperatures, but this performance drops rapidly at higher operating temperatures.

In the system, SCs and a HP deliver heat to a hot water storage tank via submerged helical heat exchangers. The final consumer flow results in the controlled mixing by a thermostatic valve of cold tap water with hot water from the storage tank. The storage temperature is maintained at 48 (°C) at the top by the solar collectors and the heat pump. SCs are active if they can gain energy with the current conditions. On the other side, the heat pump's control system is set to be active if the solar collectors are not capable to maintain the HWST temperature.

Configuration A characterize itself for having a double evaporator HP, of which it can use just one at the time. The first evaporator allows the HP to use air as its heat source. On the other side, the second evaporator allows the HP to work as a water-water HP where the heat source fluid corresponds to the SC's working water. Then, configuration A has two modes of operation:

- Parallel operation: heat from the SCs is used directly in the HWST. If the HP is activated, it uses its air-source evaporator.
- Series operation: heat from the SCs is used indirectly, as a heat source for the HP. Thus, the HP uses its water source evaporator. In this mode, collectors are chilled, and the HP works with a higher temperature source.

It is important to notice that no simultaneous mode of operation can occur; the system works either as in parallel or in series mode. Configuration A's architecture and overall control strategy of each individual component is shown in Figure 2.

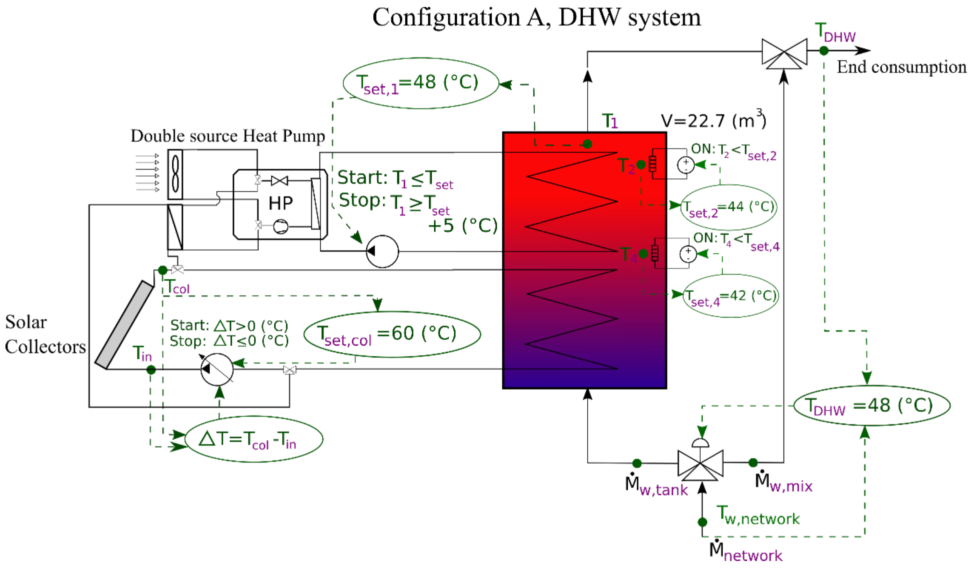

Figure 2: Simplified scheme of the components and hydronics of the DHW system in A configuration.

On its side, B configuration replaces the double source HP by a more conventional air-source HP. This time, the HP has a heat exchanger that can warm its heat source air using the SC's heat. Thus, two modes of operation can commute. As in A configuration, no partial parallel/series operation is permitted. Configuration B's architecture and overall control strategy of each individual component is shown in Figure 3.

- Parallel in B configuration: The system operates in the exact same way that the parallel operation of the A configuration.
- Series in B configuration: The collector's flow is redirected towards the heat exchanger to pre-heat the air passing through the HP evaporator.

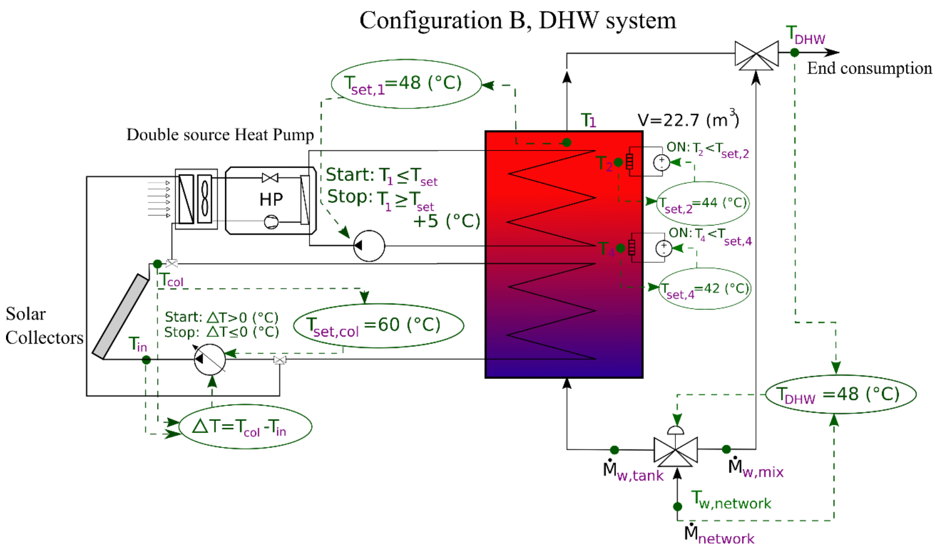

Figure 3: Simplified scheme of the components and hydronics of the DHW system in B configuration.

4.2. Equipment sizing.

DHW system has been designed based on the heat loads of the mid-rise residential building. It has been established than the maximum capacity required to maintain the internal energy of a HWST is of 84 kW for the climate of Puerto Montt. Then, the system in its A and B configuration is designed with a HP somewhat oversized that can supply the heat demand in case there is no heat contribution by the SCs. A 90 kW HP is chosen and a total SC area in the range of t. Nonetheless, preliminary simulations, not shown in this paper for the sake of brevity, show that at some times desired DHW is not in the desired temperature, so two auxiliary heaters are installed. The auxiliary heaters capacities are chosen to diminish considerably this problem. On the other hand, the HWST volume sizing is chosen so it can store approximately the total daily consumption of the mid-rise residential building. The geometry of the tank is taken from the most suitable commercially available equipment found.

Table 3: Main components sizing of the DHW SHP system.

Nominal A7W30 heat pump's capacity (parallel mode)	Collectors-area/heat-pump-capacity ratio	Total solar collectors área	HWST volume	Auxiliary electric heaters capacity
90 kW	2.5	225 m^2	22.7 m^3	6 kW (x2)

4.3. System components modelling

4.3.1. Particularities on the Heat Pump modelling

A detailed physical model of heat pump is developed for TRNSYS 17. Its objective is to permit the authors further work in modelling SHP systems that require to simulate the refrigerant thermodynamical states in dynamic simulations. Nonetheless, this model is not finally implemented in the presented TRNSYS simulations and a black-box model whose performance map is obtained by testing the physical model in steady-state conditions replaces it.

The physical model code compiled in 4 TRNSYS modules that interact in its kernel: a condenser model, an air source evaporator model, a water source evaporator model and a compressor model.

The compressor model is based on its volumetic and isentropic efficiencies. Thus, the mass flow rate and the power consumption by the compressor are described in equations (1) and (2).

$$\dot{m}_{ref} = \dot{V}_{swept} * \rho_{in,comp} * \eta_{vol} \tag{1}$$

$$\dot{W}_{el,comp} = \dot{m}_{ref} * \frac{h_{out,comp,s} - h_{in,comp}}{\eta_s} \tag{2}$$

On the other side, the volumetric and isentropic efficiencies depend mainly on the pressure ratio of the compressor. The efficiencies are modelled as in equations (3) and (4).

$$\eta_s = K_1 + K_2\left(r_p - R_1\right)^2 - \frac{K_3}{r_p - R_2} \tag{3}$$

$$\eta_{vol} = a_0 - \alpha * r_p \tag{4}$$

Where $K_1, K_2, K_3, R_1, R_2, a_0$ and α are constants calculated from data from a compressor's catalogue.

On the other hand, heat exchangers are modeled accordingly to algorithms found in the literature survey, such as Type 877 described by Heinz & Haller (2013). Each heat exchanger working conditions are calculated with the inlet flow rates, inlet temperatures and total area of heat exchange. Global heat transference coefficient U is calculated with correlations that uses mass flow rate. UA_{HXis} then determined. Then, the HX is divided into sections accordingly to different refrigerant states: superheated gas, liquid-gas mixture and subcooled liquid. In each section, a local UA_i coefficient is calculated according to equation (5).

$$UA_i = \frac{\dot{Q}_i}{\Delta T_{log,i}} \tag{5}$$

Subcooling and superheating temperatures are assumed constant. The total heat transferred in the gas-liquide mixture section of the HX is calculated iterating the condensation or evaporation pressures, accordingly to the type of HX. Thus, convergence on the iteration of condensation or evaporation pressure is reached when equation (6) is fulfilled.

$$\sum UA_i = UA_{HX} \tag{6}$$

This physical model is not yet optimized at the time of writing this article. Nonetheless, the authors used this model to design a heat pump. Aiming for future work in the Space Heating simulations based in the residential building case study, 9 kW of nominal capacity is aimed. The selected compressor for designing and modelling the heat pump of the SH system is Copeland ZH38K4E, whose working fluid is R134a. The heat exchangers characteristics were chosen in order to maximize COP at nominal conditions, reaching 4.31. After design, the heat pump model is tested in steady state conditions to create a performance map under different heat source and heat sink temperatures, using both an air source evaporator and a water source evaporator. Thus, the performance data is used with commercial black box heat pump models that simulate the heat pump's energy consumption and heating capacity.

Table 4: Adjusted parameters to calculate the isentropic and volumetric efficiencies of the Copeland ZH38K4E compressor in the physical model.

K_1	K_2	K_3	R_1	R_2
0,388402	0,0011285	0,147789	20	1,3
a_0	α	V_{swept} (cm^3)	RPM (1/s)	
1,03195	0,0155827	82,76	2900	

For modelling the DHW system heat pump, the same performance map is used, but with a scale factor of 10 to adjust the heating capacity and power consumption for a 90 kW heat pump.

4.3.2. Modules used in each SHP system component.

For the system modelling, several modules available in TRNSYS and from Thermal Energy System Specialists [23-28] have been used. The most important components used in the system model are listed in Table 5.

Table 5: Models used in TRNSYS for the SHP systems simulation. Corresponding documentation is mentioned in references.

Type number	Description	Description/Parameters
538	Evacuated Tubes Collector Model	Quadratic efficiency curve model. Parameters: η_0=0.642; a_1=0.885; a_2=0.001. Bi-angular IAM's extracted from TESS library.
1290	Unglazed solar collector	Quadratic efficiency curve model. Parameters: η_0=0.828; a_1=18.52; a_2=0. b_0=0.1.
941	Air-to-Water Heat Pump	This model is based on an user-supplied performance map of the modelled heat pump containing the capacity and power consumption for various operating temperatures.
927	Water-to-Water HP. Used when the system works in series operation in configuration A	This model is based on an user-supplied performance map of the modelled heat pump containing the capacity and power consumption for various operating temperatures.
534	Cylindrical Storage Tank (with immersed heat exchangers in the DHW system)	Constant volume, fluid filled tank model. The stratification is modelled through isothermal nodes. 10 vertical nodes. In the DHW system, there are internal coiled tubes HXs. Heat loss coefficient on every surface of 3 [$kJ\cdot h^{-1}\cdot m^{-2}\cdot K^{-1}$].

The solar collector's coefficients for their modelling are obtained from commercially available catalogue data of Wolf CRK-12 (ETC) and Heliocol HC-30 (UC). Their efficiency curves are shown in Figure 4. It can be seen the UC has more efficiency potential but a reduced operational range.

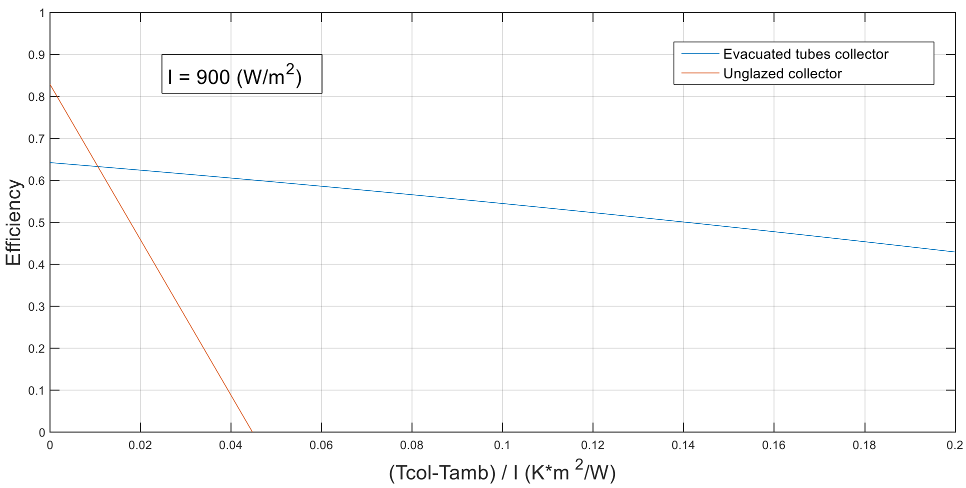

Figure 4: Efficiency curves of both evacuated tubes collector and unglazed collector used.

4.4. Control system for the mode of operation mode switching.

The control system designed switches the operation mode of each system mainly according to the total solar radiation available on the collectors' surface G_{col}. Thus, the control system of both system in A configuration requires 4 conditions for the system to operate in series, presented in Table 6.

Table 6: Conditions of the control system for activating series operation mode for systems in A configuration.

If the available solar radiation on the collector's surface fulfills	If the solar collectors are running:	If the inlet water temperature of the heat pump's evaporator fulfills:	If the heat pump is activated :
$G_{col} < G_{lim,control}$	$T_{out,col} > T_{in,col}$	$T_{in,evap,HP} > 2\ (°C)$	$*T_1 < T_{1,set}$

$*T_1$ is the top tank temperature, as shown in Figures 2&3.

The control system for both systems in B configuration also needs 4 conditions to switch to indirect solar use, showed in Table 7.

Table 7: Conditions of the control system for activating series operation mode for systems in B configuration.

If the vailable solar radiation on the collector's surface fulfills:	If the solar collectors are running:	If the solar collectors are running:	If the heat pump is activated:
$G_{col} < G_{lim,control}$	$T_{out,col} > T_{in,col}$	$T_{out,col} > T_{amb} + 1\ (°C)$	$*T_1 < T_{1,set}$

$*T_1$ is the top tank temperature, as shown in Figures 2&3.

Both systems layouts are simulated through a whole TMY with different setups of $G_{lim,control}$, in order to search for a value that could improve SPF_{syst}. For every case study, 6 $G_{lim,control}$ values are tested, ranging from 0 and 500 W/m^2 with an increasing pace of 100 W/m^2. Notice that at $G_{lim,control}$= 0 W/m^2, the system operates exclusively in parallel mode.

5. Simulation results and discussion.

5.1. Performance figures definitions.

Every simulation is performed within a timestep of 2 minutes for a period of one TMY. Analysis will be carried according to the following performance figures and definitions.

$$\mathrm{SPF_{syst}} = \frac{\int \dot{Q}_{DHW} \cdot d\tau}{\int (\dot{W}_{el,tot,pp} + \dot{W}_{el,tot,HP} + \dot{W}_{el,tot,aux}) \cdot d\tau} \tag{7}$$

$$\mathrm{SPF_{HP}} = \frac{\int \dot{Q}_{u,HP} \cdot d\tau}{\int \dot{W}_{el,tot,HP} \cdot d\tau} \tag{8}$$

$$\mathrm{F_{sol}} = \frac{\int \dot{Q}_{u,col,HWST} \cdot d\tau}{\int (\dot{Q}_{u,col} + \dot{Q}_{u,HP} + \dot{W}_{el,tot,aux}) \cdot d\tau} \tag{9}$$

$$\eta_{ave,col} = \frac{\int \dot{Q}_{u,col} \cdot d\tau}{\int G_{col} \cdot A_{col} \cdot d\tau} \tag{10}$$

Notice F_{sol} consider solar heat when in direct use and $\eta_{ave,col}$ in both parallel and series operation. Also, the free energy fraction, defined as the renewable energy heat fraction delivered to the HWST can be calculated as in equation (11).

$$F_{free} = \frac{\int \dot{Q}_{free} \cdot d\tau}{\int (\dot{Q}_{u,HP} + \dot{Q}_{u,col,HWST} + \dot{W}_{el,tot,aux}) \cdot d\tau} = \frac{\int \dot{Q}_{free} \cdot d\tau}{} \tag{11}$$

$$\begin{aligned} \int \dot{Q}_{free} \cdot d\tau &= \int \left(\dot{Q}_{u,col} + \dot{Q}_{airHP}\right) \cdot d\tau = \int \left(\dot{Q}_{u,col,HWST} + \dot{Q}_{HP,evaps}\right) \cdot d\tau \\ &= \int \left(\dot{Q}_{u,col,HWST} + \dot{Q}_{u,HP} - \dot{W}_{el,tot,HP}\right) \end{aligned} \tag{12}$$

5.2. DHW system results.

Thirty-six simulations are executed for assessing A and B configurations in the 3 selected cities and for diferent $G_{lim,control}$ sets. SPF_{syst} is the most relevant parameter to conclude and compare system performance. Its predicted values are presented in Figure 5. It is important to notice that for a set of $G_{lim,control}$=0, A and B configuration work exclusively in parallel and with the same components sizing. Thus, for the same city weather and assessed type of solar collector both simulation should show the same results. This is not the case, and slightly different SPF_{syst} are encountered in each couple of theoretically equal results. The average difference in SPF_{syst} is of 0.15, while the largest relative difference is 4.84%; thus, the authors consider it is not a relevant matter because the true interest is in the figure dependence with $G_{lim,control}$. The authors attribute this to numerical deviations in the TRNSYS kernel because of different modules connections.

5.2.1. Components analysis.

Component analysis is essential to understand the overall system behaviour. First, it is important to notice that in every case study the SPF_{HP} figure increases with $G_{lim,control}$. These results are to be expected for A and B configurations, because the HP works more frequently with a higher temperature source if series mode is activated more often. Also, it is important to notice that in A configuration, for the same operating temperatures, the water source evaporator improves heat pump's COP because of better heat transfer efficiency than with air.

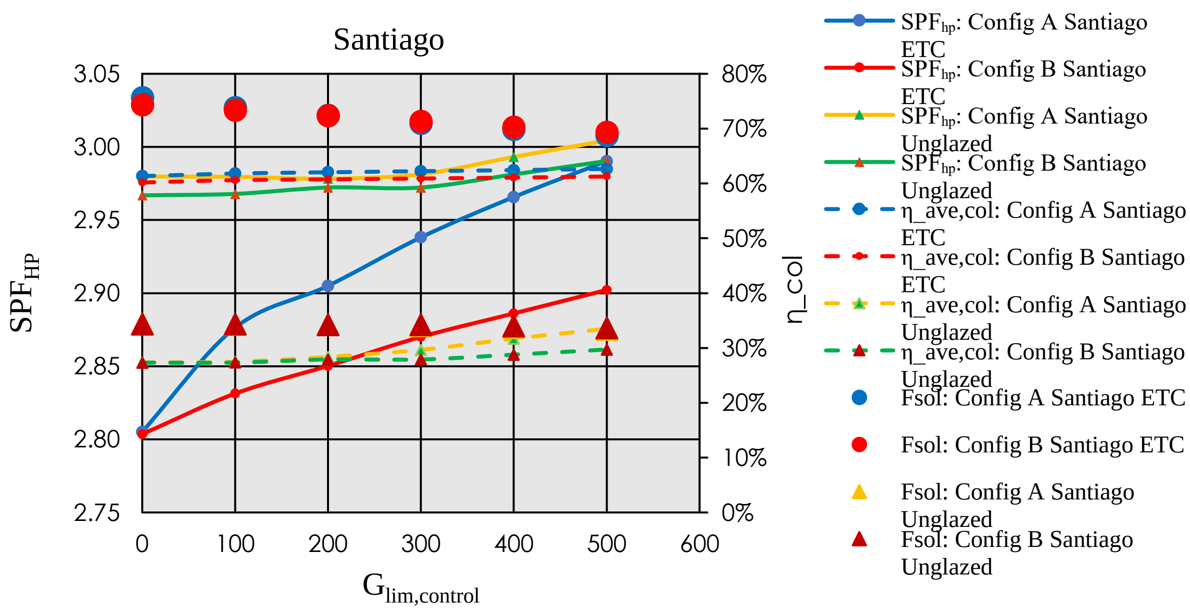

(a)

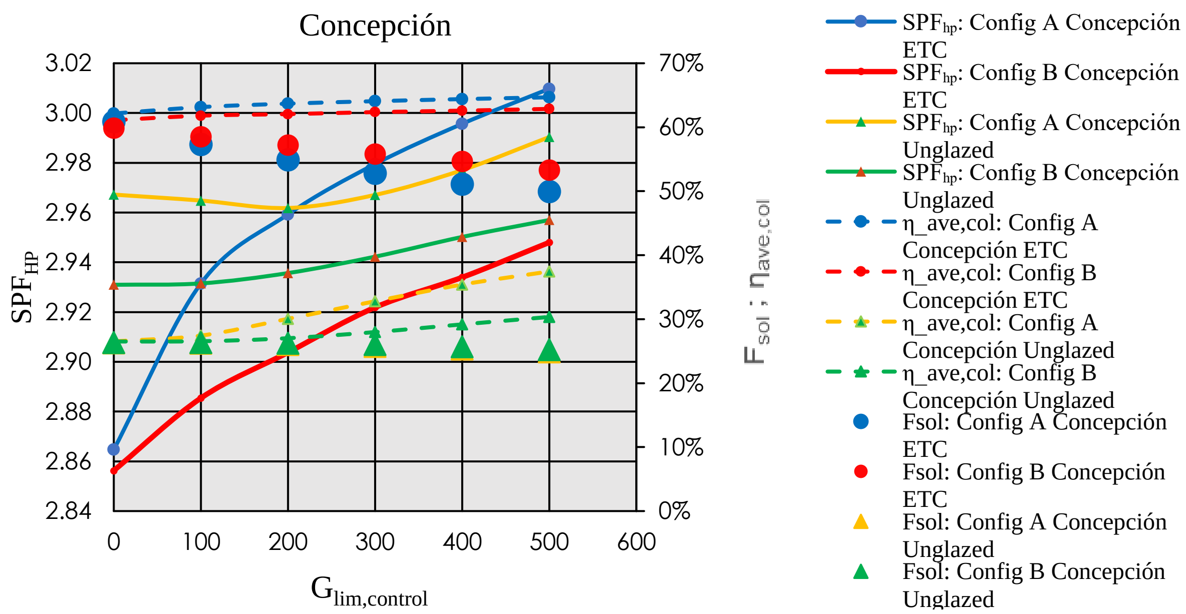

(b)

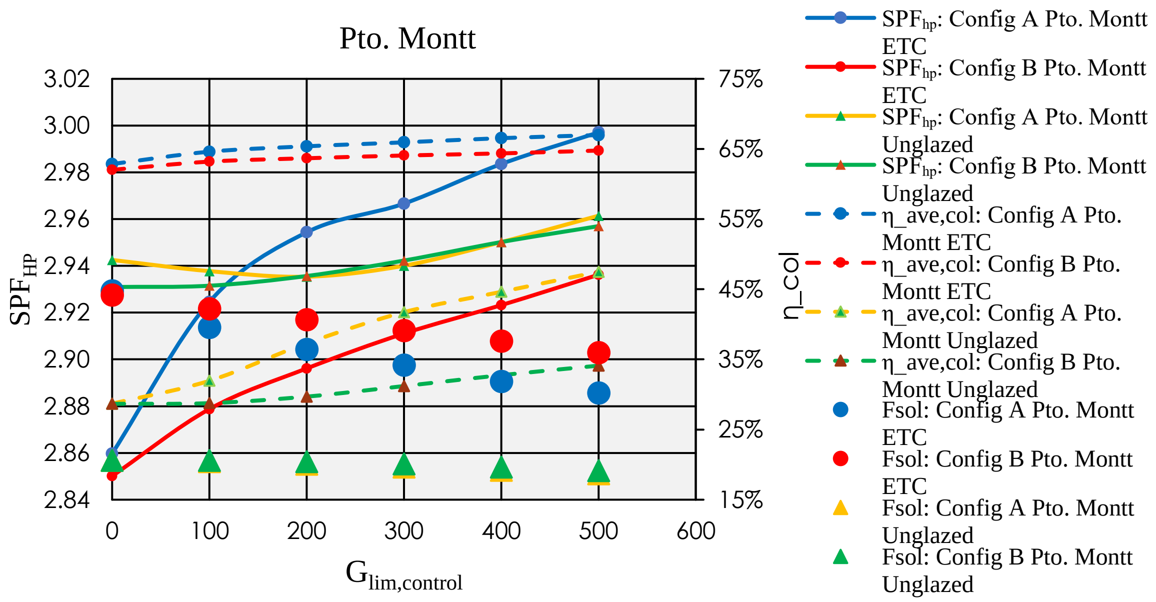

(c)

Figure 5: SPF_{HP} , F_{sol} and $\eta_{ave,col}$ for each case study in the climates of (a) Santiago, (b) Concepción and (c) Puerto Montt in the DHW system.

A comparative analysis between SPF_{HP} tendencies show that A configuration has the better relative increase of this figure, reaching a 6.6% rise for Santiago's climate using ETCs. On its side, B configuration only manages to improve SPF_{HP} in 3.5% for the same climate and SCs. For each scenario, as expected, the double source HP appears as the best option to improve the component's performance, as shown in Table 8.

Table 8: Relative increase of each SPF_{HP} in the DHW system. Base value is obtained with $G_{lim,control} = 0$.

Configuration	SC	Santiago	Concepción	Puerto Montt
A	ETC	6.6%	5.1%	4.8%
	UC	0.82%	0.78%	0.64%
B	ETC	3.5%	3.2%	3.0%
	UC	0.79%	0.84%	0.89%

Regarding the $\mathrm{SPF_{HP}}$ improvement with each SC type, it is found that ETCs are the ones that increases the most the performance figure. This is explained by two factors. First, as seen in Figure 5, ETC have a wider range of operation; thus, they can support the HP more often since possible additional runtimes than UCs are covered. Second, contrary to what may be expected, $\eta_{ave,col}$ of UC did not surpassed ETC's even if the purpose of the system was to seize their low temperature potential efficiency.

Nonetheless, performance figures of both type of SCs did improve with $G_{lim,control}$. However, ETCs didn't show considerable relative improvement of $\eta_{ave,col}$. For this type of SCs, they consistently improve more their performance in A configuration, reaching a maximum increase of 4.13% for Puerto Montt's climate. As it is expected, UCs improve considerably more they performance, but not surpassing the ETC's. Again, A configuration is the one who achieves better improvement, reaching 18.8% in Puerto Montt. It is also important to notice that the performance increases more if the climate is colder because greater convectional heat losses are avoided, especially with UCs. Results are shown in Table 9.

Table 9: Maximum increase of $\eta_{ave,col}$ for each case study in the DHW system.

Configuration	SC	Santiago	Concepción	Puerto Montt
A	ETC	1.31%	2.53%	4.13%
	UC	6.16%	10.93%	18.80%
B	ETC	1.09%	1.77%	2.75%
	UC	2.4%	3.84%	5.44%

The second figure that describes collectors' behaviour is F_{sol}. When increasing series mode operation range, less solar heat is used directly for charging the HWST. Thus, the figure is expected to decrease with $G_{lim,control}$, as shown in Table 10.

Table 10: Maximum decrease of F_{sol} for eachcase study in the DHW system.

Configuration	SC	Santiago	Concepción	Puerto Montt
A	ETC	-6.86%	-10.93%	-14.55%
	UC	-0.97%	-1.4%	-1.9%
B	ETC	-5.04%	-6.55%	-8.25%
	UC	-0.71%	-1.07%	-1.45%

5.2.2. Global system analysis.

SPF_{syst} results for each of the simulations are presented in Figure 6.

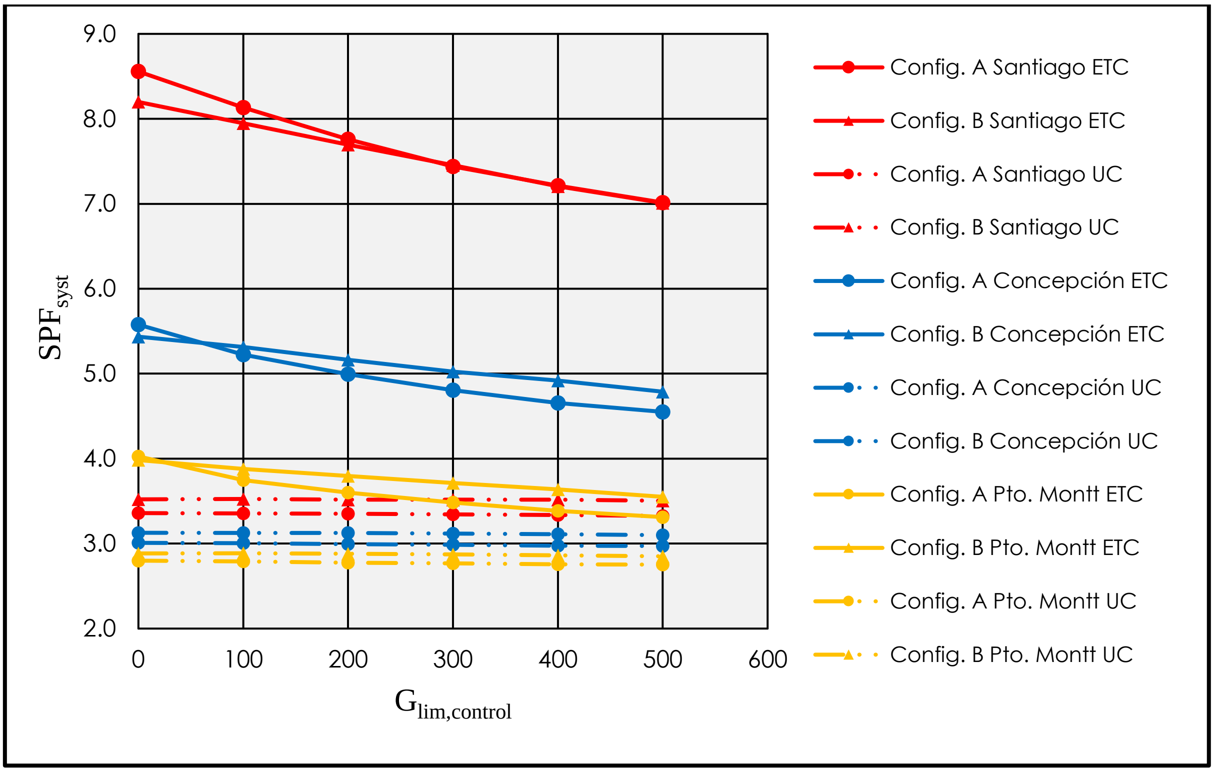

Figure 6: SPF_{syst} of A and B configurations of the DHW system in function of $G_{lim,control}$ set

On the main facts to notice, Puerto Montt is the city where constantly SPF_{syst} is the lowest for each configuration and SC type assessed. This is to be expected because it's the climate with the least solar irradiation and the lowest average ambient temperature, thus affecting negatively the SCs performance and the HP's COP. Lowest system performance figure for $G_{lim,control}$=0 W/m^2 is obtained in Puerto Montt with A configuration and UC, reaching a 2.8 value. The lowest SPF_{syst} of all is predicted for the same conditions with $G_{lim,control}$=500 W/m^2.

On the contrary, for the inverse reasons, the best SPF_{syst} are found in the Santiago climate. For the system operating exclusively in parallel, best results are found in A configuration using ETC, reaching a value of 8.56. In the surveyed literature, such high figures where never found. This is partly explained by the fact that most literature's case studies are in colder cities with least solar irradiation. Nonetheless, the main reason of this is that the SC total area has not been adjusted according to each climate and it is probably more economically reasonable to lower it for Santiago's climate. Even if a sensibility analysis for determining economically optimal SC areas is not relevant for testing this paper's thesis, it is seen as a work perspective.

Regarding the thesis put to test, it is observed that for each assessed configuration, type of SC used and climate, SPF_{syst} decreases with increasing $G_{lim,control}$. In other words, if the control system sets a wider range of operation conditions for the series mode, the system performs worst. Thus, it is verified that the control system, cannot improve the DHW system performance even if it based on the available solar irradiation. But, if individual performance figures of both SC and HP increases with $G_{lim,control}$, what explains the decrease of SPF_{syst}? In the case of A configuration, the increase of $\eta_{ave,col}$ and SPF_{HP} do not compensate the fact that when the system operates in series mode, it uses just one energy source (solar), when it could be using two energy sources at the same time (solar and air) in parallel mode. On its side, when B configuration operates in series it uses free energy from both air and solar collectors. Nonetheless, when this happens, the solar heat transferred to the HP's evaporator is done in expense of an energy quota that otherwise would be extracted from surrounding air. This is translated in a decrease of the free energy fraction in most case studies, as shown in Figure 7. On the other hand, Figure 8 shows that in both A and B configuration, the sum of total annual energy transferred to the HWST from the SCs and the heat pump tends to decrease up to 2.51%.

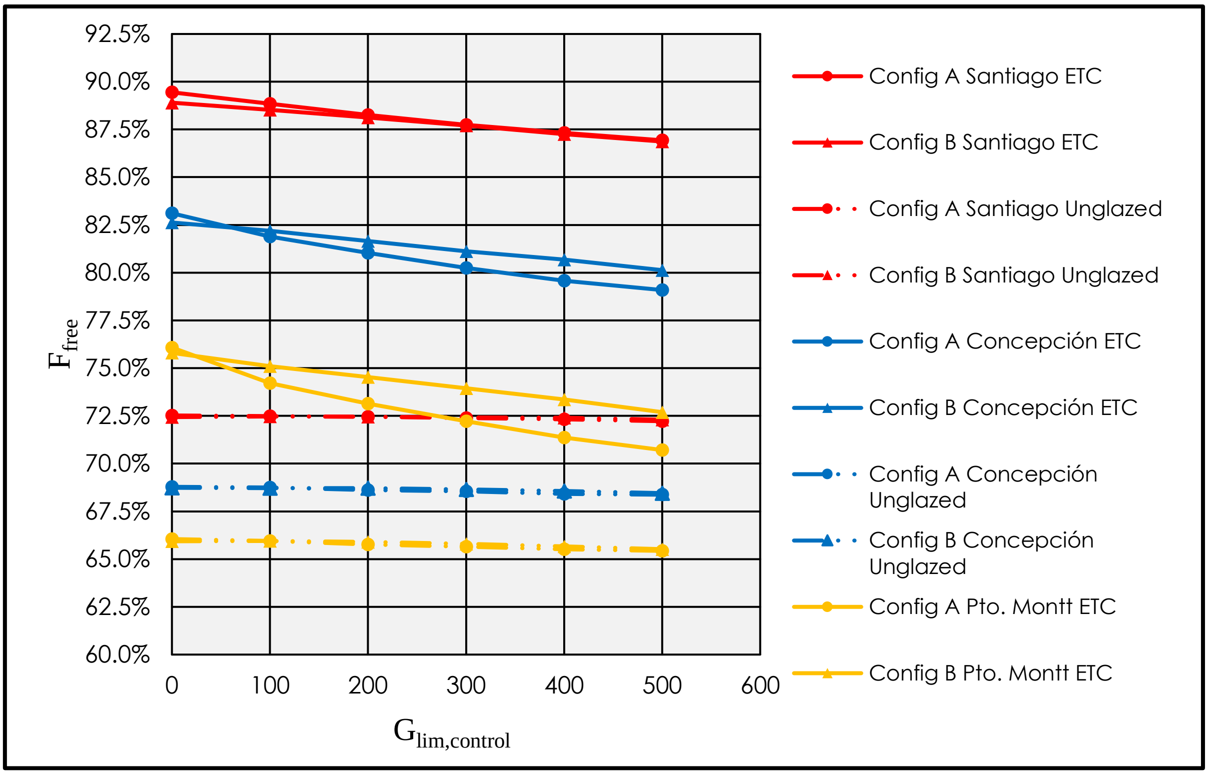

Figure 7: Free energy fraction transferred to the HWST

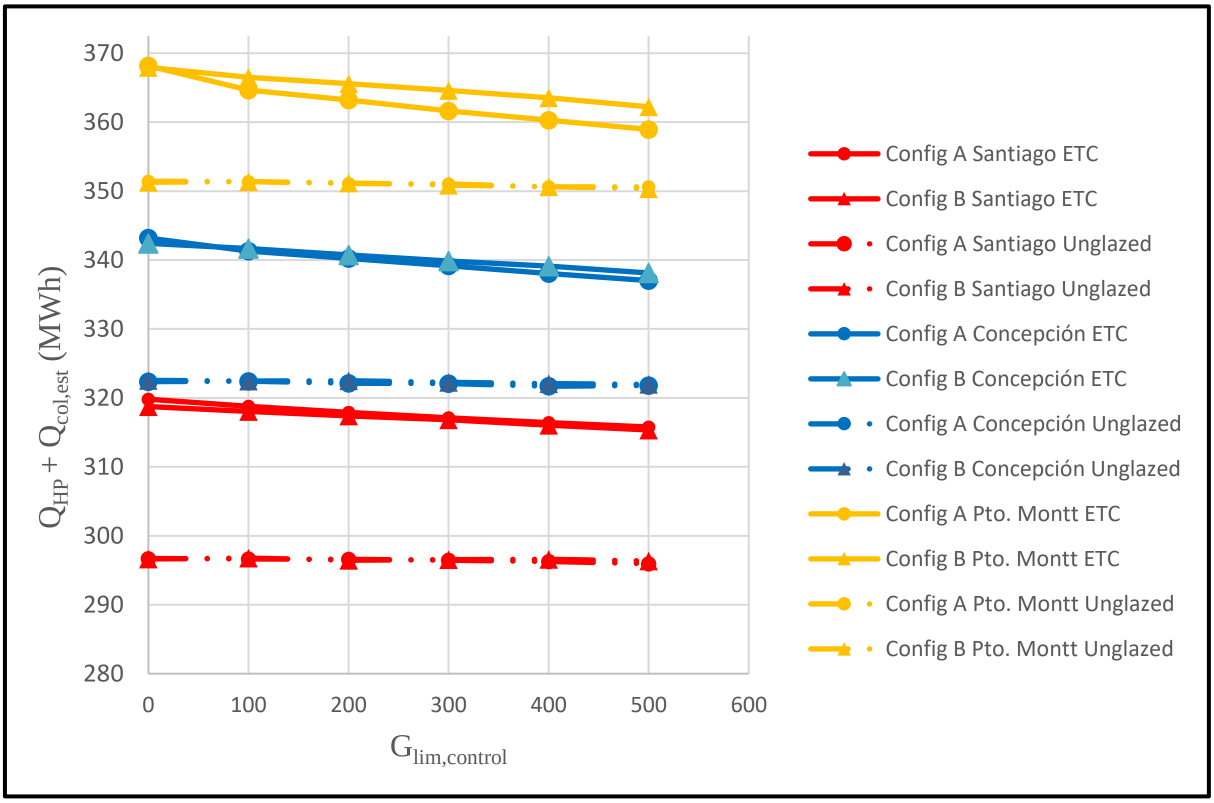

Figure 8: Total annual energy transferred to the HWST from the heat pump and the solar solar collectors in the DHW system.

This decrease on energy quota from the main system components is enough to set the auxiliary heaters running more often to maintain the defined minimum temperatures on the HWST. Thus, increasing $G_{lim,control}$ rises the amount of electric consumption, decreasing SPF_{syst}. These results are shown in Figure 9. Combined effects shown in Figure 7 and Figure 9 explain why the applied control system decreases SPF_{syst} in the DHW system.

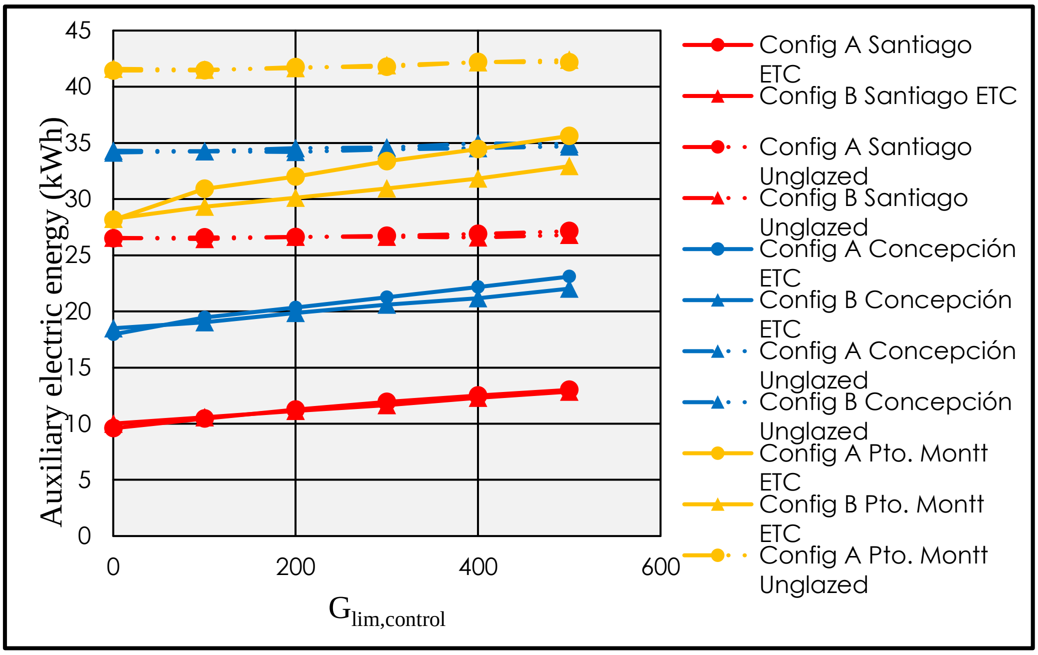

Figure 9: Total annual heat supplied by the auxiliary electric heaters of the DHW system for each case study.

It is also important to notice that for each case studied, the DHW system has better SPF_{syst} when using ETCs than with UCs. According to literature, it was expected to find a considerable performance increase on UCs when operating in series more frequently and this was not achieved. Results can be explained by the fact that the control of operation mode still has unused solar radiation potential. In other words, solar collectors' runtimes could be increased furthermore by turning ON the series mode of operation when the collectors are not previously working. This would chill them and force them into operating conditions with positive efficiency.

6. Conclusions and work perspectives.

The ability to commute between parallel and series operation, meaning direct or indirect use of solar heat, has been assessed in a solar and heat pump system with two different configurations. On one hand, a dual source (air and solar) heat pump layout has been implemented. According to literature, this configuration is beneficial if the control system decides which heat source to use in function of the available solar irradiation. In the present work, focus has been put in testing the configuration using a control system of this nature. The same is applied to a second configuration, denoted B, where the solar collectors can be used to warm the working fluid of an air source heat pump. The chosen methodology permits to test the thesis in different load temperatures, climates, magnitude order of the heat demand, heat demand profile and used solar collector type. Results show that individual performance figures increase of both heat pump and solar collectors is not a sufficient condition to improve the overall system performance figure SPF_{syst}. The reason for this is that the free energy fraction diminishes when increasing the series mode range of operation because the extra solar energy gained is lower than the air source energy the heat pump would extract in parallel operation. In other words, in evaluated systems, for both A and B configurations, there is not a limit solar irradiation below which series operation is beneficial. In fact, SPF_{syst} tends to decrease in most case studies.

Special discussion is done regarding the fact that there is still unused solar irradiation available than the series mode of operation could seize. Thus, the most important work perspective that arise in this work is the execution of numerical simulations of the same system layouts, in the same climates, using a control system that switches the mode of operation allowing the SCs to achieve all their potential runtimes. This would be done by forcing them to lower their temperature by chilling them with the HP when they were not previously working. Then, the SCs would be driven to reach a temperature where they meet a positive efficiency. Care should be taken to not allow this when there is no available solar energy, as in that condition the heat pump would perform better just taking heat from the air. A secondary work perspective is the economical and sensitivity analysis of the sizing of every main component implemented in the modelling. SHP systems are sensible to climate conditions and heat loads; thus, having additional information of the performance of these systems whose implementation is on the arise in Chile would be of interest.

Acknowledgements

This study was funded by the Chilean research agency CONICYT through the research project FONDECYT 1150965.

NOMENCLATURE

SHP	Solar and heat pump	**Subscripts**	
DHW	Domestic hot water	*lim*	Limit
COP	Coefficient of performance	*control*	Control system
F	Fraction	*syst*	System
HP	Heat pump	*ref*	Refrigerant
SC	Solar collector	*swept*	Swept
SPF	Seasonal performance factor	*vol*	Volumetric
IEA	International energy agency	*el*	Electric
SHC	Solar heating and cooling	*comp*	Compressor
SH	Space heating	*out*	Outlet
HWST	Hot water storage tank	*in*	Inlet
ASHRAE	American society of heating, refrigerating and air-conditioning engineers	*s*	Isentropic
		p	Pressure
ASPE	American society of plumbing engineers	*i*	inth therm
		log	Logarithmic
ETC	Evacuated tubes collector	*HX*	Heat exchanger
UC	Unglazed collector	*col*	Collector, collectors
IAM	Incidence angle modifier	*evap*	Evaporator
HX	Heat exchanger	*HP*	Heat pump
TMY	Typical meteorological year	*Set*	Set on the control system
		amb	Ambient
G	Solar radiation, $W \cdot m^{-2}$	*u*	Useful
$\dot{m}$	Flow rate, $kg \cdot s^{-1}$	*tot*	Total
ρ	Density, $kg \cdot m^{-3}$	*aux*	Auxiliary
$\dot{V}$	Volumetric flow rate, $m^3 \cdot s^{-1}$	*sol*	Solar
$\dot{W}$	Power, W	*DHW*	Domestic hot water
h	Enthalpy	*ave*	Average
r	Ratio	*free*	Free renewable energy
K, R, a	Constant coefficient		

U Global heat transference coefficient, $W \cdot K^{-1} \cdot m^{-2}$	**Greek symbols**
A Area, m^2	Δ Delta, difference
$\dot{Q}$ Heat flow, $W \cdot s^{-1}$	η Efficiency
T Temperature, K	α Constant coefficient
	τ Time, s

REFERENCES

Vega J., Cuevas C. Simulation study of a combined solar and heat pump system for heating and domestic hot water in a medium rise residential building at Concepción in Chile. Applied Thermal Engineering 2018; 141:565-578.

Ruschenburg J, Herkel S, Henning H. A statistical analysis on market-available solar thermal heat pump systems. Solar Energy 2013; 95:79-89.

Carbonell D., Philippen D., Granzotto M., Haller M.Y. Simulation of a solar-ice system for heatin applications. System validation with one-year of monitoring data. Energy and Buildings 126 (2016) 846-858.

Hadorn J. Solar and heat pump systems for residential buildings. First edition. Berlin: Ernst & Sohn GmbH & Co; 2015.

Fraga C., Hollmuller P., Mermoud F., Lachal B. Solar assisted heat pump system for multifamily buildings: Towards a seasonal performance factor of 5? Numerical sensitivity analysis based on a monitored case study. Solar Energy 146 (2017) 543-564.

Sun X., Dai Y., Novakovic V., Wu J., Wang R. Performance comparison of direct expansion solar-assisted heat pump and conventional air source heat pump for domestic hot water. Energy Procedia 70 (2015) 394-401.

Sterling S.J., Collins M.R. Feasibility analysis of an indirect heat pump assisted solar domestic hot water system. Applied Energy 93 (2012) 11-17.

Liu H., Jiang Y., Yao Y. The field test and optimization of a solar assisted heat pump system for space heating in extremely cold area. Sustainable Cities and Society 13 (2014) 97-104.

Poppi S, Bales C, Heinz A, Hengel F, Chèze D, Mojic I, Cialani C. Analysis of system improvements in solar thermal and air source heat pump combisystems. Applied Energy 2016; 173:606-623.

Tzivanidis C, Bellos E, Mitsopoulos G, Antonopoulos K, Delis A. Energetic and financial evaluation of a solar assisted heat pump heating system with other usual heating systems in Athens. Applied Thermal Engineering 2016; 106:87-97.

Kamil Kaygusuz. Performance of Solar-Assisted Heat-Pump Systems. Applied Energy (1995) 93-109.

Lerch W., Heinz A., Heimrath R. Direct use of solar energy as heat source for a heat pump in comparison to a conventional parallel solar air heat pump system. Energy and Buildings 100 (2015) 34-42.

Renato M. Lazarrin. Dual source heat pump systems: Operation and performance. Energy and Buildings 52 (2012) 77-85.

Haller M, Frank E. On the potential of using heat from solar thermal collectors for heat pump evaporators. ISES Solar World Congress, 28. August-2 September 2011, Kassel, Germany.

Heinz A., Haller M. Model of Sub-components and Validation for the IEA SHC Tas 44/HPP Annex 38; A3 Description of TRNSYS Type 877 by IWT and SPF. Solar Heating & Cooling Programme (SHC), International Energy Agency (IEA).

Banister C, Collins M. Development and performance of a dual tank solar-assisted heat pump system. Applied Energy 2015; 149: 125-132.

He W, Hong X, Zhao X, Zhang X, Shen J, Ji J. Operational performance of a novel heat pump assisted solar façade loop-heat-pipe water heating system. Applied Energy 2015; 146: 371-382.

Meteotest, Meteonorm Version 7, Bern, Switzerland, http://www.meteonorm.com/, 2015.

ASHRAE Standard 90.2, Energy efficient design of low-rise residential buildings. American Society of Heating, Refrigerating and Air Conditioning Engineers, Atlanta, USA, 2007.

Domestic Water Heating Design Manual, American Society of Plumbing Engineers (ASPE), 2003.

TRNSYS 17 Mathematical Reference, TRNSYS 17 Documentation, Madison, Wisconsin, USA.

Thermal Energy Systems Specialists, Solar Library Mathematical Reference, Component Libraries for the TRNSYS Simulation Environment, Madison, Wisconsin, USA, Madison, Wisconsin, USA, 2012.

Thermal Energy Systems Specialists, HVAC Library Mathematical Reference, Component Libraries for the TRNSYS Simulation Environment, Madison, Wisconsin, USA, 2012.

Thermal Energy Systems Specialists, Storage Tank Library Mathematical Reference, Component Libraries for the TRNSYS Simulation Environment, Madison, Wisconsin, USA, 2012.